Published in final edited form as:
Acta Biomater. 2013 January ; 9(1): 4806–4814. doi:10.1016/j.actbio.2012.09.020.

Hidden contributions of the enamel rods on the fracture resistance of human teeth

M. Yahyazadehfar[a], **Devendra Bajaj**[b], and **Dwayne D. Arola**[a,c,*]

[a]Department of Mechanical Engineering, University of Maryland Baltimore County, Baltimore, MD 21250, USA

[b]Department of Orthopedics, University of Medicine and Dentistry of New Jersey, New Jersey Medical School, Newark, NJ 07103, USA

[c]Department of Endodontics, Prosthodontics, and Operative Dentistry, Dental School, University of Maryland, Baltimore, MD 21201, USA

Abstract

The enamel of human teeth is generally regarded as a brittle material with low fracture toughness. Consequently, the contributions of this tissue in resisting tooth fracture and the importance of its complex microstructure have been largely overlooked. In this study an experimental evaluation of the crack growth resistance of human enamel was conducted to characterize the role of rod (i.e. prism) orientation and degree of decussation on the fracture behavior of this tissue. Incremental crack growth was achieved in-plane, with the rods in directions longitudinal or transverse to their axes. Results showed that the fracture resistance of enamel is both inhomogeneous and spatially anisotropic. Cracks extending transverse to the rods in the outer enamel undergo a lower rise in toughness with extension, and achieve significantly lower fracture resistance than in the longitudinal direction. Though cracks initiating at the surface of teeth may begin extension towards the dentin–enamel junction, they are deflected by the decussated rods and continue growth about the tooth's periphery, transverse to the rods in the outer enamel. This process facilitates dissipation of fracture energy and averts cracks from extending towards the dentin and vital pulp.

Keywords

Crack growth; Enamel; Fracture toughness; Strength

1. Introduction

Dental enamel, the outermost tissue of the human tooth, undergoes repeated contact as a result of routine mastication. Cyclic contact stresses can cause fatigue and facilitate the development of damage or cracks at the tooth's surface. This type of damage may also develop by a traumatic blow or sharp contact. Though cracks are routinely visible on the surface of teeth [1–3], they are generally arrested prior to reaching a state that enables tooth fracture. Most of the credit for this remarkable quality has been given to the interfacial region between the dentin and enamel known as the dentin–enamel junction (DEJ) [4–8].

*Corresponding author at: Department of Mechanical Engineering, University of Maryland Baltimore County, Baltimore, MD 21250, USA. Tel.: +1 410 455 3310; fax: +1 410 455 1052. darola@umbc.edu (D.D. Arola).

Potential contributions of the enamel in preventing tooth fracture have received limited attention.

Cracks in enamel that are initiated by sharp indentation normal to the occlusal surface of teeth exhibit Palmqvist geometry and undergo extension parallel or perpendicular to the rod axes [9]. Both crack paths involve extension in-plane with the enamel rods, a keyhole shaped structure comprising an assembly of nanometer-scale carbonated hydroxyapatite crystallites (~25 nm thick, ~100 nm wide and ≫ 100 nm long) that are aligned predominately along the longitudinal axis, except for within the interrod region [10]. The rods, also often regarded as prisms, are outlined by a very thin "sheath" ($t \ll 1$ μm) of non-collagenous organic matrix and extend between the DEJ and occlusal surface. In the "outer" enamel (closest to the tooth's surface) the rods extend in a nearly parallel arrangement from just beneath the occlusal surface inward. Approximately midway between the tooth's surface and DEJ, i.e. within the "decussated" enamel, the rods extend within alternating "bands" that follow a sinusoidal path; adjacent bands are oriented obliquely to one another [11,12]. This complex microstructure undoubtedly plays an important role on the direction of crack extension within enamel and on the tooth's resistance to growth.

There has been interest in the fracture behavior of enamel for many decades. Many evaluations have utilized indentation techniques for estimating the "apparent" fracture toughness, and reported values ranging from roughly 0.4 to 1.5 MPa·$m^{0.5}$ [7,9,13–15], which are, in general, lower than those of the other mineralized tissues [16,17]. Xu et al. [14] found the apparent toughness of occlusal enamel (0.77 ± 0.05 MPa·$m^{0.5}$) to be larger than at the buccal-lingual surface (0.52 ± 0.06 MPa·$m^{0.5}$). Park et al. [9] evaluated variations across the thickness and found an increase in the apparent toughness and decrease in the brittleness of enamel from the occlusal surface to the DEJ. The largest gradient in these measures of mechanical behavior was observed in old enamel (patient age ≥ 50 years), which exhibited significantly higher brittleness and lower apparent toughness than those properties of younger teeth.

Due to concerns with the indentation approach [18,19], recent studies concerning the fracture resistance of enamel have adopted a conventional fracture mechanics approach [20–22]. The initiation toughness for human enamel from this approach ($0.52 \leq K_0 \leq 0.83$ MPa·$m^{0.5}$) is reportedly within the range of estimates from indentations [20]. However, there is a substantial rise in crack growth resistance with extension (beyond a factor of three), which is largely attributed to the crack path within the region of rod decussation. Human enamel exhibits rising R-curve behavior for cracks extending from the occlusal surface inwards and in the reverse direction, i.e. from the DEJ outward [21]. Those extending from the occlusal surface inwards exhibit greater stability, suggesting that enamel has been designed to arrest cracks that begin at the tooth's surface. Surprisingly, the R-curve behavior for cracks extending perpendicular to the rods in human enamel has not been examined.

In the present investigation we explore the role of enamel and its microstructure in preventing tooth fracture from cracks that initiate at the tooth's surface. The fracture behavior of human enamel was evaluated for crack extension in two orthogonal directions, i.e. from the occlusal surface inwards toward the dentin and vital pulp, and transverse to this direction about the tooth's circumference. The evaluation examines differences in the mechanisms of toughening in the two directions and identifies how they support the damage tolerance of human teeth.

2. Materials and methods

Caries-free human third molars were obtained from participating clinics in the state of Maryland according to an approved protocol (Y04DA23151) issued by the Institutional Review Board of the University of Maryland Baltimore County. The teeth were stored in Hanks's balanced salt solution (HBSS), with age and gender recorded. All teeth were obtained from patients between 17 and 25 years of age.

Within 1 month of extraction, selected teeth were sectioned using a numerical controlled slicer/grinder under water-based coolant using diamond abrasive slicing wheels. Sectioning (Fig. 1(a)) was performed to obtain $2 \times 2 \times 2\text{mm}^3$ cubes of cuspal enamel (one from each tooth). Not all sectioned teeth possessed a cusp thickness that supported obtaining the desired $2 \times 2 \times 2\text{mm}^3$ cube, in which case the tooth was discarded. For those teeth with adequate cusp thickness, the sectioning was performed with great care to obtain the desired enamel entirely without dentin. The sectioned enamel cubes were then molded within a commercial dental resin composite (Vit-l-escence, Ultra dent Products, Inc., South Jordan, UT, USA) according to Fig. 1(b). Detailed descriptions of bonding and placement of the inset have been described elsewhere [20,23,24]. The molded sections were further processed to achieve a compact tension (CT) geometry, including a back channel (1 mm deep) and two holes to enable Mode I cyclic loading. Note that the reduction in enamel thickness at the back channel was used to reduce the opening mode load necessary to achieve crack growth while maintaining an acceptable surface area for bonding of the enamel inset. Lastly, a chevron notch was prepared using a razor blade and diamond paste. The enamel inset orientation was chosen to achieve crack growth along the axis of the rods in the longitudinal orientation ($n = 11$) or in the transverse direction ($n = 15$). The results for six of the samples with longitudinal orientation of crack growth were reported in an earlier evaluation focused on the fracture behavior and toughening mechanisms of human enamel [20]. Thus, five additional specimens were evaluated and the results combined for increasing the samples size and statistical power. For specimens with transverse orientation, sectioning was performed to achieve crack growth limited to the outer enamel (closest to occlusal surface) or in the inner enamel (adjacent to DEJ), as shown in Fig. 1(c).

Fatigue loading of the CT specimens was performed using a commercial testing frame (Enduratec, Model 3100, Eden Prairie, MN, USA) to develop a well-defined crack (~0.3 mm long) from the prepared notch. Stable crack growth experiments were performed using a dedicated universal testing system complemented with microscopic imaging system. Quasi-static loading was conducted with 1 N increments until the onset of crack extension, followed thereafter using 0.5 N load increments until the point of instability. Hydration of the samples was maintained during loading using a saturated cotton swab "cradle" that was nestled beneath the specimen and retained moisture from an eyedropper of HBSS. Digital images were acquired during each stage to identify the displacement field and crack lengths using digital image correlation (DIC). A detailed description of the microscopic DIC process and its application is given elsewhere [25]. In short, the crack opening displacement distributions were used to precisely identify the crack tip from the location of zero opening-mode displacement. Then, the opening mode stress intensity (K_I) distribution was calculated using the crack length measurements according to [20]

$$K_I = \frac{P}{B^* \sqrt{W}} \sqrt{\frac{B^*+1}{B+1}} (1.69 - 8.01\,\alpha + 12.53\,\alpha^2)\ (\text{MPa} \cdot m^{0.5}) \quad (1)$$

where P is the opening load (Newtons), α is the ratio of a to W, B (mm) is the specimen thickness and B^* (mm) is the specimen thickness adjacent to the back channel as illustrated in Fig. 1(b).

To evaluate whether enamel exhibits anisotropic fracture resistance, it was necessary to characterize the crack growth behavior in the transverse orientation in the outer enamel and decussated regions separately. However, due to the complexity of the decussated enamel and the specimen preparation process, it was impossible to obtain cubes that were exclusively outer enamel without decussation. Therefore, the fracture surfaces of all specimens were examined post-testing using a scanning electron microscope (SEM; JEOL JSM 5600, JEOL Inc., Peabody, MA) in secondary electron imaging mode. Measurements of the depth of prism decussation were made on the fracture surface as a function of crack length, as shown in Fig. 2. Using these measurements, the degree of prism decussation (D) was estimated according to the ratio of decussated fracture area (A^*) to total fracture area (A), and was calculated from the initiation of stable crack extension to a specified crack length. The numerical value of D was estimated according to

$$D=\frac{A^*}{A}=\frac{\int_0^{a'} t_d \cdot dx}{\int_0^{a'} t \cdot dx} \quad (2)$$

where t_d and t are the width of decussated fracture area and total fracture area, respectively (Fig. 2). The integration is performed from the initiation of stable growth along the crack growth direction. Note that the crack length (a') is defined here from the onset of crack extension and not from the load-line indicated in Eq. (1). Characterization of D enabled the critical stress intensity distribution for the specimens with transverse orientation to be classified as either outer or inner enamel, and quantitatively in terms of the degree of decussation.

The influence of prism decussation on the crack growth behavior, path of crack extension and mechanisms of toughening were also evaluated by examining fractured and additional partially tested specimens using the aforementioned SEM in backscatter emission imaging mode. For selected specimens, monotonic crack extension was discontinued prior to fracture for observation of the intact crack path. To enhance the microstructure, the crack face was etched using 34% phosphoric acid for 25 s, polishing with 3 μm and 0.1 μm diamond suspensions, and then ultrasonically cleaned. Thereafter, the specimens were coated with gold–palladium before evaluation with the SEM.

3. Results

Crack extension within the enamel specimens extended from the notch and continued along a path that was primarily perpendicular to the loading direction in all samples evaluated. The preferred path of crack extension coincided with the plane of maximum opening mode stress intensity. Stable crack growth was achieved over a length of between 1 and 2 mm in both orientations, and an increase in the applied driving force was required to achieve incremental extension to the point of gross fracture.

Typical load vs. opening displacement curves for quasi-static crack growth in the transverse orientation within specimens of inner and outer enamel are shown in Fig. 3(a). There are two distinct regions in the load distributions corresponding to an elastic response (Region I) prior to crack extension, and a secondary region (Region II) associated with incremental crack extension until the point of instability. Crack growth within the samples of outer enamel

typically initiated at opening loads of $3 \leq P \leq 4$ N, approximately half that required for the specimens of inner enamel ($5 \leq P \leq 8$ N); crack extension within the longitudinal direction generally occurred for $4 \leq P \leq 6$ N. A crack growth resistance curve (i.e. R-curve) developed from the incremental load and crack length response for transverse crack growth within inner enamel is shown in Fig. 3(b). Each of the growth responses was characterized in terms of the initiation toughness (K_0), the rise in toughness with crack extension or "growth" toughness (K_g) and maximum crack growth resistance (i.e. fracture toughness, K_c). Regardless of orientation, there was no distinct plateau in the fracture resistance curves. Therefore, K_c was quantified from the maximum value of stress intensity captured at the point of unstable fracture. Crack growth resistance curves obtained from all specimens in the longitudinal and transverse directions of crack growth are shown in Fig. 3(c).

There was a marked increase in the fracture resistance with crack extension in both directions of crack growth. The average initiation, growth and plateau toughness obtained from the resistance curves in the two directions are listed in Table 1. There was no significant difference ($p > 0.05$) in the measures of initiation toughness in the two directions. However, the average growth ($p \leq 0.05$) and maximum toughness ($p \leq 0.01$) for crack extension in the longitudinal direction were significantly greater than those values obtained for the transverse direction. From a comparison of the R-curves and the values listed in Table 1, it was noted that the transverse responses exhibited a larger degree of variation. For example, the range in apparent fracture toughness for transverse crack growth exceeded a factor of two, with $1.01 \leq K_c \leq 2.41$ MPa·m$^{0.5}$. The range for the longitudinal direction was far lower, with $1.75 \leq K_c \leq 2.37$ MPa·m$^{0.5}$. A similar observation regarding the variability in transverse crack growth resistance was reported in an earlier evaluation of fracture in bovine enamel [22].

To establish the relative importance of microstructure on the toughening behavior, results for samples in the transverse direction were divided into those prepared with respect to the occlusal surface (outer enamel; $n = 9$) and the DEJ (inner enamel; $n = 6$) regions. These two locations correspond to the non-decussated and decussated regions, respectively. Average values for the fracture resistance parameters are listed in Table 1. When examined in this manner, the outer enamel exhibited a significantly lower resistance to the initiation of crack growth and a less substantial rise in toughness with crack extension. Similarly, the maximum resistance to crack growth of the outer enamel was significantly lower ($p \leq 0.01$) than that within the inner decussated region. Therefore, for the transverse direction all three components of the crack growth resistance are significantly greater within the decussated region closest to the DEJ.

Despite having prepared samples with the intention of evaluating non-decussated and decussated enamel independently, observation of the fracture surfaces revealed that there was some variability in the extent of decussation amongst samples of inner and outer enamel. The non-uniformity in decussation boundary with distance from the occlusal surface caused most inset CT specimens to be composed of a combination of straight and decussated rods. Selected samples exemplifying those with the lowest and highest degree of decussation are shown in Fig. 4(a) and (b), respectively. In each of these figures the decussation boundary is highlighted. Due to potential contributions of the variation in microstructure, the degree of decussation (D) was estimated for each specimen as a function of crack length according to Eq. (2). The R-curves presented for the transverse direction in Fig. 3(c) are presented in Fig. 4(c) with the inclusion of D. It is important to highlight that the experimental data in this figure represents over 150 points, and was obtained from the crack growth resistance curves for the 15 transverse enamel specimens. As evident from this distribution, the rise in toughness was strongly influenced by the degree of decussation. Samples of inner enamel with the highest degree of decussation underwent the largest

increase in toughness with crack extension. The overall largest rise in toughness (K_c/K_0 = 3.3) was achieved by the sample with the largest degree of decussation (0.85).

Using the quantitative description for degree of decussation, the samples with transverse prism orientation were ranked according to their D values. Samples with the lowest degree of decussation ($D \leq 30\%$, $n = 5$) and those with the highest degree of decussation ($D \geq 70\%$, $n = 5$) were selected to characterize the innermost and outermost enamel, respectively. These two groups are perhaps most representative of transverse crack growth in the non-decussated and fully decussated enamel, respectively. Results for the quantitative measures of fracture resistance for these two groups are shown in Fig. 5(a–c), along with results for the longitudinal orientation. There was a significant difference ($p \leq 0.005$) in the average K_0 between the longitudinal and transverse directions, as evident in Fig. 5(a). The overall lowest resistance to the initiation of crack extension was for transverse crack growth in the outer enamel. In examining the estimates for K_g (Fig. 5(b)), the largest degree of crack growth toughening occurred for the samples with longitudinal orientation; the average K_g for this direction (2.48 ± 1.11 MPa·m$^{0.5}$ mm^{-1}) was significantly greater ($p \leq 0.05$) than for transverse crack growth, regardless of depth. Furthermore, the K_c for transverse crack growth in the outer enamel (1.23 ± 0.20 MPa·m$^{0.5}$) was significantly lower ($p \leq 0.001$) than that for inner enamel, or in the longitudinal direction. However, there was no significant difference between the fracture toughness for transverse crack growth in the inner enamel or for crack extension in the longitudinal direction.

Spatial variations in the fracture behavior signified potential differences in the mechanisms of toughening and/or their potency. Representative transverse crack growth paths in the outer and inner enamel are presented in Fig. 6(a) and (b), respectively. In both regions the crack paths followed the plane of maximum opening mode stress intensity, with only subtle changes in primary orientation. While the preferred path of growth is along the weaker and highly organic inter-prismatic spaces amongst the prism boundaries, crack growth did occur within the rods, as evident from the insets presented at higher magnification. Within the outer enamel, the most prominent mechanisms of toughening are crack bifurcation and branching, which often served as a precursor to the generation of unbroken ligaments comprising relatively small bundles of rods (5–10). Within the inner enamel the crack path was comparatively more tortuous and largely influenced by the decussation patterns, as viewed in Fig. 6(b). Though there was a lower degree of crack branching observed in the inner enamel, crack bridging was more dominant and consisted of larger unbroken ligaments (comprising between 10 and 50 individual rods). In many cases the bridges were exposed by secondary cracks that appeared to extend backwards from the primary crack, as evident in Fig. 6(b). It is expected that these features are a result of the threedimensional nature of the crack geometry, as the crack proceeds on different planes amongst adjacent bundles of decussated rods. Note that the unbroken ligaments within the inner enamel most commonly developed at locations of transition between the diazone and parazone regions. Crack extension in the longitudinal direction undergoes toughening through a number of mechanisms, including microcracking, crack curving and crack bridging, the majority of which develop at the transition into the decussated region and continue to develop until the crack reaches the DEJ. These mechanisms, and their relative importance, have been discussed in detail elsewhere [20] and operate across the length scales noted by Ang et al. [26].

4. Discussion

In this investigation the importance of prism orientation and degree of decussation on the fracture behavior of human enamel were evaluated. Crack growth resistance curves were obtained for stable crack growth in-plane with the rods and in directions longitudinal and

transverse to the prism axes. These are the most predominant paths for cracks initiating at the occlusal surface of human teeth. Results obtained for the transverse orientation are the first reported measures obtained for human enamel from a conventional fracture mechanics approach. Overall, it was found that both directions of crack extension exhibited rising R-curve behavior, as evident in Fig. 3(c). While the resistance to the initiation of fracture (K_0) was not dependent on orientation, there were significant differences in the degree of toughening per unit crack extension (K_g) and in the apparent fracture toughness (K_c) in the two directions (Table 1). Both the K_g and K_c were highest for the longitudinal direction, i.e. where extension occurs along the axis of the rods and is directed towards the dentin and vital pulp.

To the authors' knowledge, this is the first investigation to interpret the fracture resistance of enamel in terms of the extent of fracture area comprising decussated rods. The definition used for describing D (Eq. (2)) is admittedly simple, but it captures a quality that is integral to the toughening behavior. As evident in Fig. 4(c), the crack growth resistance distributions are strongly influenced by D, and those samples with the largest values exhibited the most potent toughening. A cross-section of a third molar is shown in Fig. 7(a), which highlights the transition between decussated and non-decussated regions. The fraction of enamel thickness that is composed of decussated rods (termed here the decussation ratio, h/H) is plotted in this figure from the cemento-enamel junction (CEJ) to the cusp. There is an increase in relative thickness of decussated enamel with proximity to the occlusal surface, a trend that has been recognized for some time [27]. This may result in a greater degree of decussation developing during crack extension. However, the significance of this variation in microstructure may have been overlooked. The distributions for K_0 and K_c associated with transverse crack growth are presented in terms of the degree of decussation in Fig. 7(b) and (c), respectively. It is important to recognize that the measures of fracture resistance in Fig. 7(c) are presented at the critical crack length, which is not a constant amongst the specimens. The initiation toughness undergoes a modest increase with D (a factor of 1.5), but the changes in K_c are more substantial. Recognizing that decussation is critical to the extent of crack growth toughening that can be achieved, it is fascinating that dimensions of the decussated region are modulated according to its expected role about the tooth's crown. The largest fraction of decussated enamel is evident in the vicinity of the cusps, which correspond to the regions of highest expected driving forces and need for retarding crack extension. One aspect of enamel decussation that has not been explored in detail is the spatial variation in decussation pattern, or differences in teeth of mammals over a range in bite force. This characteristic may also be an important aspect of nature's design that is used to tune the fracture behavior, and is a topic for future study.

Bechtle et al. [22] recently evaluated the Mode I and Mode II fracture resistance behavior of enamel from bovine incisors for cracks extending in the two directions evaluated here. In that study rising R-curve behavior was noted in both directions, with values for the initiation ($0.8 \le K_0 \le 1.5$ MPa·m$^{0.5}$) and peak ($2 \le K_c \le 4.4$ MPa·m$^{0.5}$) toughness that generally agree with those values for human enamel (Table 1). Crack extension in the bovine enamel was achieved over approximately 0.5 mm length, which translates into a larger K_g than achieved for human enamel. Though the initiation toughness is not dependent on the specimen type [28], crack growth toughening is generally greater in the bending configuration due to differences in the bridging stress intensity factor [29]. Thus, the use of two different specimen configurations can be a source for the dissimilarity in apparent toughening behavior between the R-curves for human and bovine enamel. Thus, direct comparison of the toughening results for bovine and human enamel is difficult.

There is an additional concern in comparing the results obtained here with previous reports. In the aforementioned study of bovine enamel [22] there was no difference in the fracture

resistance behavior between longitudinal and transverse crack growth. That observation conflicts with the present findings. There are a number of plausible explanations for this difference. Of primary importance, in the teeth of different mammals there are variations in the enamel thickness [30,31] and degree of decussation [32], the latter of which is a critical factor according to the substantial importance of the degree of decussation (Figs. 4(c) and 7(b and (c)). In addition, bovine enamel exhibits unique fibril-like structures and a greater degree of interprismatic material in comparison to human enamel [33]. Moreover, the evaluation of bovine enamel was conducted under Mode I loading but promoted mixed-mode fracture, with a specific ratio of Mode I and Mode II loading. In the longitudinal direction the mixed-mode crack path appeared to result from differences in the enamel prism orientation with respect to the plane of opening mode stress; the cracks were simply guided by the organic interface, which served as the "weak link". For transverse crack growth, however, the authors attributed the preferred mixed-mode extension as arising from the effects of the hydroxyapatite crystal orientation in the interrod region and shearing of proteins about the rod sheaths. Both are plausible mechanisms. Within the human enamel, crack advance was dictated by the maximum opening mode stress, and occurred along the interprismatic regions via elongation and fracture of the interfacial proteins in tension.

Drawing help from the measures of fracture resistance in the two directions (Fig. 5), it is possible to comment on the fate of cracks that undergo initiation at the occlusal surface and the importance of the enamel microstructure. In examining the initiation toughness, there is a significant difference between the values for K_0 in the longitudinal and transverse directions. This suggests that cracks would be more likely to undergo extension transversely, about the tooth's periphery. However, the ratio of initiation toughness for the longitudinal and transverse directions considering cracks beginning at the occlusal surface is not large (1.25), indicating a rather moderate degree of anisotropy. Thus, depending on the nature of indentation and the driving force, cracks could proceed in either of the two directions along the protein-rich interprismatic paths. Both paths follow the rods, deterring the crack from returning to the occlusal surface and preventing the development of surface craters through chipping, which may serve later as venues for oral bacteria or sites that undergo rapid degradation. Under sufficient driving force, the crack would continue to extend along the rods until it exhausts the available energy, or until it reaches the decussated enamel. Here is where the hidden contributions of enamel become evident in resisting tooth fracture. If the crack is to continue to extend in the longitudinal direction, it must overcome the high growth toughness (Fig. 5(b)). The alternative involves a continuation of growth in the transverse direction. The ratio of the growth toughness in the longitudinal and transverse directions is 1.3 when performed using the K_g for the inner enamel. If that ratio is estimated using the K_g for transverse crack growth for outer enamel, it exceeds a factor of 2 (2.4). Consequently, the crack path requiring the least energy for further extension is transverse to the rods. The disparity in growth toughness between the two directions serves to deflect the crack and discourage its progression towards the DEJ. This mechanism also enables further dissipation of fracture energy through transverse crack growth that is restricted to the outer enamel. This is undoubtedly a reason why cracks are seen about the surface of teeth but do not lead to tooth fracture. In instances where the driving force is large enough to exceed the mechanisms of toughening and the crack proceeds in the longitudinal direction, the DEJ will serve as the second defense in preventing bulk fracture [4–7,9].

This investigation focused on the fracture behavior of enamel for cracks that initiate at the occlusal surface under sharp contact or fatigue damage. That is not the only origin or cause of tooth failure; it may also result from very large occlusal forces generated during mastication, which has been studied quite extensively [34–36]. In human teeth, large occlusal forces often cause tensile hoop stresses about the margins within the enamel shell, and appear to facilitate the initiation of cracks at the tufts [37], a protein-filled fissure or

defect extending from the DEJ [11]. The mechanics of fracture and critical failure loads under these conditions are topics that extend far beyond the realm of enamel as a biomaterial, and have anthropological implications [3]. Nevertheless, important studies in this area have helped in establishing that the load-bearing capacity of teeth is largely a function of tooth geometry and enamel thickness [38,39]. In these investigations the estimates for critical load to fracture of enamel have been based on a constant value of crack growth resistance ($K_c < 1$ MPa·m$^{0.5}$). The authors acknowledge that variations in the enamel thickness and degree of prism decussation could complicate the formation and extension of cracks. Results from the present study (Fig. 7) could serve as a valuable resource for future estimates of such behavior.

Scientists are now engineering the microstructure of materials with combinations of ceramic and polymeric constituents by freezing [40]. These microstructures have been inspired by those of natural materials, including bone and nacre, and are achieving fracture toughnesses that are more than two orders of magnitude greater than the constituents [41,42]. Recognizing the potential for utilizing a microstructure to guide cracks or to deflect cracks towards regions that are less threatening, it appears that there are lessons to be learned from enamel. However, it is important to point out that this evaluation was restricted to an examination of the roles of prism orientation and decussation on the fracture behavior. The prism assembly and its orientation is also important to the apparent “plastic deformation” of enamel at the microscopic [30] and nanoscopic scales [43,44].

With all studies there are potential limitations, and the present investigation is no exception. Results of this evaluation were obtained for the cuspal enamel of selected human third molars that were obtained from patients of a relatively young age. The mechanical behavior of enamel undergoes changes with age [9,45], which could be important to anisotropy in the fracture behavior and the nature of inhomogeneity. There are also potentially unknown factors related to the health status, diet or oral hygiene of the donors that could contribute to variability in the crack growth behavior. Another important concern is that the enamel evaluated in this investigation was obtained from the cusps of teeth that are not enrolled in mastication. Moreover, while no attention was placed on whether the tissue was obtained from the buccal or lingual cusp, there are differences in the chemical composition of enamel from different regions of the tooth, and this factor is important to the bulk mechanical properties [46–48]. An evaluation of the differences in degree of decussation and chemical composition between molars that are enrolled in mastication and those that are not has not been performed. These factors could play an important role on the fracture behavior of human enamel and are topics reserved for future study.

5. Conclusions

An experimental evaluation of the fracture resistance of human enamel was conducted for crack extension occurring in-plane with the rods and in two orthogonal directions (i.e. longitudinal and transverse to the prism axes). Based on results from this investigation, the following conclusions were drawn:

1. Human enamel exhibits rising R-curve behavior for crack extension occurring in the longitudinal and transverse directions. In both the inner and outer enamel, the preferred path of crack extension in both directions is along the protein-rich interface of adjacent rods, rather than within intrarod region.
2. The lowest resistance to the initiation of crack growth ($K_0 = 0.54 \pm 0.1$ MPa·m$^{0.5}$) was obtained for cracks extending transverse to the rods in the outer enamel (nearest the occlusal surface). The largest value of K_0 (0.83 ± 0.07 MPa·m$^{0.5}$) was obtained for transverse crack growth within the inner enamel.

3. The largest rise in crack growth resistance with crack extension (K_g = 2.48 ± 1.11 MPa·m$^{0.5}$ mm^{-1}) and the largest apparent fracture toughness (K_c = 2.01 ± 0.21 MPa·m$^{0.5}$) were obtained for cracks extending parallel to the axis of the rods and within the inner (i.e. decussated) region. Conversely, the lowest growth toughness (K_g = 1.05 ± 0.26 MPa·m$^{0.5}$ mm^{-1}) and apparent fracture toughness (K_c = 1.23 ± 0.20 MPa·m$^{0.5}$ mm^{-1}) were obtained for transverse crack growth in the outermost enamel.
4. The crack growth resistance of human enamel exhibits both anisotropy and inhomogeneity. The combination of these two qualities appears to arise from the complexity of the hierarchical microstructure and the decussated prism structure. Most importantly, the decussation of enamel causes a deflection of cracks extending from the enamel surface inwards, but simultaneously facilitates a continuation of transverse crack extension within the outer enamel. This process deters cracks from reaching the dentin or pulp, a path most likely to result in tooth fracture.

Acknowledgments

This study was supported in part by the National Institutes of Dental and Craniofacial Research through grant (R01 DE016904). The authors would also like to thank Ultradent Products Inc for supplying the Vit-l-escence resin composite.

References

1. Abou-Rass M. Crack lines: the precursors of tooth fractures – their diagnosis and treatment. Quintessence Int Dent Dig. 1983; 14:437–47. [PubMed: 6574554]
2. Xu HHK, Kelly JR, Jahanmir S, Thompson VP, Rekow ED. Enamel subsurface damage due to diamond tooth-preparation. J Dent Res. 1997; 76:1698–706. [PubMed: 9326903]
3. Lucas PW, Constantino PJ, Wood BA, Lawn BR. Dental enamel as a dietry indicator in mammals. BioEssays. 2008; 30:374–85. [PubMed: 18348196]
4. Lin CP, Douglas WH. Structure-property relations and crack resistance at the bovine dentin–enamel junction. J Dent Res. 1994; 73:1072–8. [PubMed: 8006234]
5. Marshall GW Jr, Balooch M, Gallagher RR, Gansky SA, Marshall SJ. Mechanical properties of the dentinoenamel junction: AFM studies of nanohardness, elastic modulus, and fracture. J Biomed Mater Res. 2001; 54:87–95. [PubMed: 11077406]
6. Dong XD, Ruse ND. Fatigue crack propagation path across the dentinoenamel junction complex in human teeth. J Biomed Mater Res A. 2003; 66:103–9. [PubMed: 12833436]
7. Imbeni V, Kruzic JJ, Marshall GW, Marshall SJ, Ritchie RO. The dentin–enamel junction and the fracture of human teeth. Nat Mater. 2005; 4:229–32. [PubMed: 15711554]
8. Bechtle S, Fett T, Rizzi G, Habelitz S, Klocke A, Schneider GA. Crack arrest within teeth at the dentinoenamel junction caused by elastic modulus mismatch. Biomaterials. 2010; 31:4238–47. [PubMed: 20167362]
9. Park S, Quinn JB, Romberg E, Arola D. On the brittleness of enamel and selected dental materials. Dent Mater. 2008; 24:1477–85. [PubMed: 18436299]
10. Robinson, C.; Kirkham, J.; Shore, R. Dental enamel: formation to destruction. Boca Raton, FL: CRC Press; 1995. p. 151-52.
11. Sognnaes RF. The organic framework of the internal part of the enamel; with special regard to the organic basis for the so-called Tufts and Schreger's bands. J Dent Res. 1949; 28:549–57. [PubMed: 15398056]
12. Ten Cate, AR. Oral histology: development, structure, and function. 7. St. Louis, MO: Mosby; 2008. p. 141-190.
13. Hassan R, Caputo AA, Bunshah RF. Fracture toughness of human enamel. J Dent Res. 1981; 60:820–7. [PubMed: 6937518]

14. Xu HHK, Smith DT, Jahanmir S, Romberg E, Kelly JR, Thompson VP, et al. Indentation damage and mechanical properties of human enamel and dentin. J Dent Res. 1998; 77:472–80. [PubMed: 9496920]
15. Padmanabhan SK, Balakrishnan A, Chu MC, Kim TN, Cho SJ. Micro-indentation fracture behavior of human enamel. Dent Mater. 2010; 26:100–4. [PubMed: 19796801]
16. Kruzic JJ, Ritchie RO. Fatigue of mineralized tissues: cortical bone and dentin. J Mech Behav Biomed Mater. 2008; 1:3–17. [PubMed: 19627767]
17. Arola D, Bajaj D, Ivancik J, Majd H, Zhang D. Fatigue of biomaterials: hard tissues. Int J Fatigue. 2010; 32:1400–12. [PubMed: 20563239]
18. Quinn GD, Bradt RC. On the Vickers indentation fracture toughness test. J Am Ceram Soc. 2007; 90:673–80.
19. Kruzic JJ, Kim DK, Koester KJ, Ritchie RO. Indentation techniques for evaluating the fracture toughness of biomaterials and hard tissues. J Mech Behav Biomed Mater. 2009; 2:384–95. [PubMed: 19627845]
20. Bajaj D, Arola D. On the R-curve behavior of human enamel. Biomaterials. 2009; 30:4037–46. [PubMed: 19427691]
21. Bajaj D, Arola D. Role of prism decussation on fatigue crack growth and fracture of human enamel. Acta Biomater. 2009; 5:3045–56. [PubMed: 19433137]
22. Bechtle S, Habelitz S, Klocke A, Fett T, Schneider GA. The fracture behavior of dental enamel. Biomaterials. 2010; 31:375–84. [PubMed: 19793611]
23. Zhang D, Nazari A, Soappman M, Bajaj D, Arola D. Methods for examining the fatigue and fracture behaviour of hard tissues. Exp Mech. 2007; 47:325–36.
24. Bajaj D, Nazari A, Eidelman N, Arola D. A comparison of fatigue crack growth in human enamel and hydroxyapatite. Biomaterials. 2008; 29:4847–54. [PubMed: 18804277]
25. Zhang D, Luo M, Arola D. Displacement/strain measurement under optical microscope with digital image correlation. Opt Eng. 2006; 45:1–9.
26. Ang SF, Schulz A, Pacher Fernandes R, Schneider GA. Sub-10-micrometer toughening and crack tip toughness of dental enamel. J Mech Behav Biomed Mater. 2011; 4:423–32. [PubMed: 21316630]
27. Skobe Z, Stern S. The pathway of enamel rods at the base of cusps of human teeth. J Dent Res. 1980; 59:1026–32. [PubMed: 6929287]
28. Fett T, Munz D, Geraghty RD, White KW. Influence of specimen geometry and relative crack size on the R-curve. Eng Fract Mech. 2000; 66:375–86.
29. Munz D. What can we learn from R-curve measurement? J Am Ceram Soc. 2007; 90:1–15.
30. Lawn BR, Lee JJ, Constantino PJ, Lucas PW. Predicting failure in mammalian enamel. J Mech Behav Biomed Mater. 2009; 2:33–42. [PubMed: 19627805]
31. Lawn BR, Lee JJ, Chai H. Teeth: among nature's most durable biocomposites. Ann Rev Mater Res. 2010; 40:55–75.
32. Lucas, PW. Dental functional morphology: how teeth work. Cambridge: Cambridge University Press; 2004.
33. Fonseca RB, Haiter-Neto F, Carlo HL, Soares CJ, Sinhoreti MAC, Puppin-Rontani RM, et al. Radiodensity and hardness of enamel and dentin of human and bovine teeth, varying bovine teeth age. Arch Oral Biol. 2008; 53:1023–9. [PubMed: 18675389]
34. Chai H, Lee JJW, Kwon JY, Lucas PW, Lawn BR. A simple model for enamel fracture from margin cracks. Acta Biomater. 2009; 5:1663–7. [PubMed: 19269906]
35. Lawn BR, Lee JJ. Analysis of fracture and deformation modes in teeth subjected to occlusal loading. Acta Biomater. 2009; 5:2213–21. [PubMed: 19268644]
36. Lee JJ, Kwon JY, Chai H, Lucas PW, Thompson VP, Lawn BR. Fracture modes in human teeth. J Dent Res. 2009; 88:224–8. [PubMed: 19329454]
37. Myoung S, Lee J, Constantino P, Lucas P, Chai H, Lawn B. Morphology and fracture of enamel. J Biomech. 2009; 42:1947–51. [PubMed: 19559438]
38. Lee JJ, Morris D, Constantino PJ, Lucas PW, Smith TM, Lawn BR. Properties of tooth enamel in great apes. Acta Biomater. 2010; 6:4560–5. [PubMed: 20656077]

39. Barani A, Keown A, Bush MB, Lee JJW, Chai H, Lawn BR. Mechanics of longitudinal cracks in tooth enamel. Acta Biomater. 2011; 7:2285–92. [PubMed: 21296195]
40. Deville S, Saiz E, Nalla RK, Tomsia AP. Freezing as a path to build complex composites. Science. 2006; 311:515–8. [PubMed: 16439659]
41. Munch E, Launey ME, Alsem DH, Saiz E, Tomsia AP, Ritchie RO. Tough, bio-inspired hybrid materials. Science. 2008; 322:1516–20. [PubMed: 19056979]
42. Launey ME, Munch E, Alsem DH, Saiz E, Tomsia AP, Ritchie RO. A novel biomimetic approach to the design of high-performance ceramic–metal composites. J R Soc Interf. 2010; 7:741–53.
43. He LH, Swain MV. Contact induced deformation of enamel. Appl Phys Lett. 2007; 90(1–3): 171916.
44. He LH, Swain MV. Understanding the mechanical behaviour of human enamel from its structural and compositional characteristics. J Mech Behav Biomed Mater. 2008; 1:18–29. [PubMed: 19627768]
45. Park S, Wang DH, Zhang D, Romberg E, Arola D. Mechanical properties of human enamel as a function of age and position in the tooth. J Mater Sci: Mater Med. 2008; 19:2317–24. [PubMed: 18157510]
46. Cuy JL, Mann AB, Livi KJ, Teaford MF, Weihs TP. Nanoindentation mapping of the mechanical properties of human molar tooth enamel. Arch Oral Biol. 2002; 47:281–91. [PubMed: 11922871]
47. Braly A, Darnell LA, Mann AB, Teaford MF, Weihs TP. The effect of prism orientation on the indentation testing of human molar enamel. Arch Oral Biol. 2007; 52:856–60. [PubMed: 17449008]
48. He LH, Swain MV. Enamel-a functionally graded natural coating. J Dent. 2009; 37:596–603. [PubMed: 19406550]

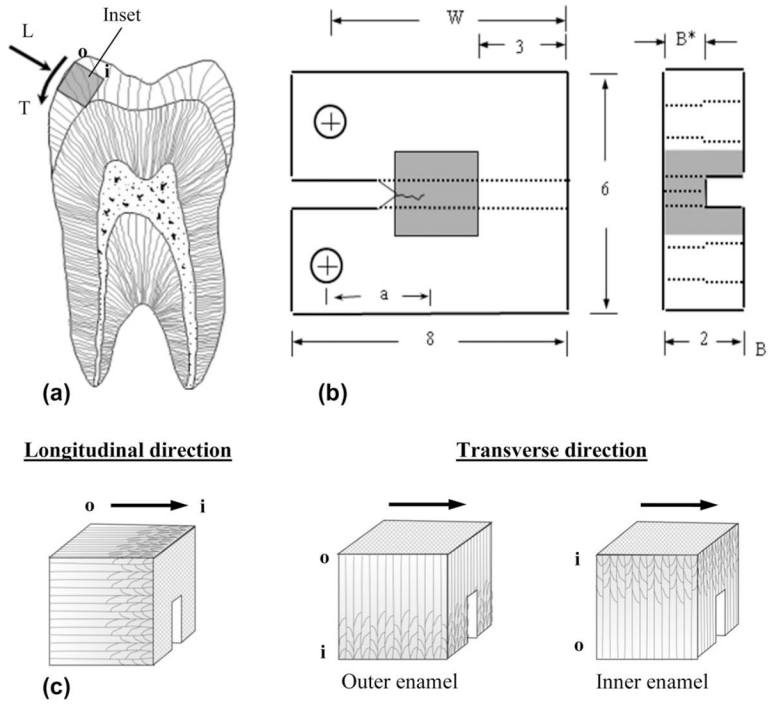

Fig. 1.

Specimen preparation, geometry and testing orientations. (a) Buccal–lingual section of molar with potential inset of occlusal enamel highlighted. Note the longitudinal (L) and transverse (T) directions of crack growth. The letters “o” and “i” refer to the outer and inner enamel, respectively. (b) Geometry of the CT specimen. The molded enamel inset is approximately $2 \times 2 \times 2\text{mm}^3$ and embodied within a dental resin composite. All dimensions are in millimeters. (c) Relative placement of the back channel in enamel inset for the longitudinal and transverse orientations directions. The arrows illustrate the path of crack growth. For the transverse direction, samples are shown for crack growth within the outer and inner enamel as indicated.

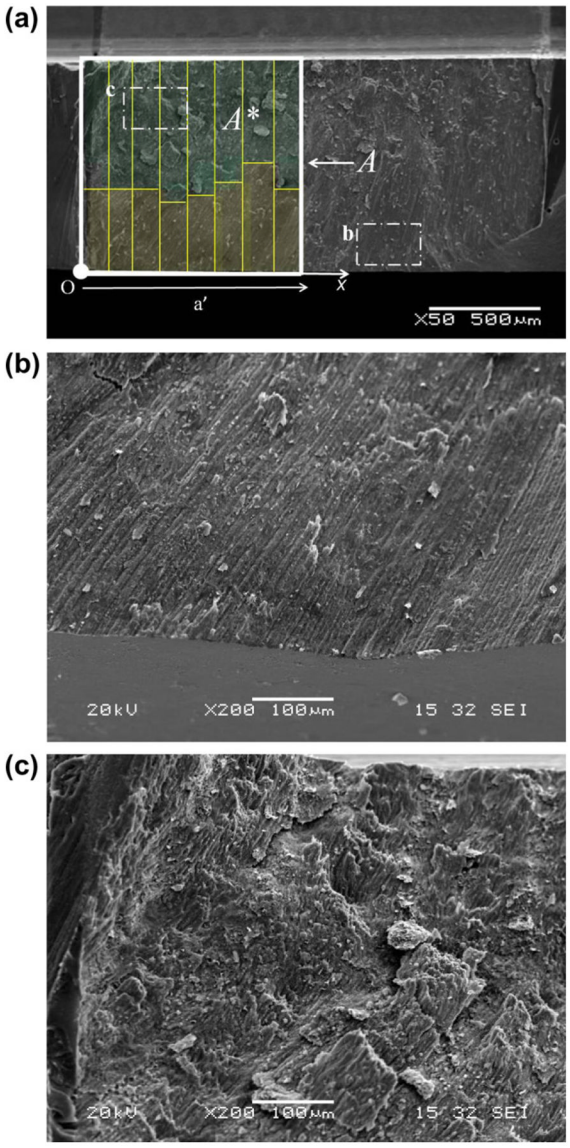

Fig. 2.

Characterizing the degree of decussation from the fracture surfaces. The direction of crack extension is from left to right. (a) SEM micrograph of a fracture surface. The rods uniformly extend from the occlusal surface (bottom) but begin to undergo decussation close to the back channel. The degree of decussation at a specific crack length is defined as the ratio of decussated fracture area A^* to total fracture area A. (b) Micrograph of non-decussated outer enamel close to occlusal surface. (c) Micrograph of heavily decussated inner enamel close to back channel.

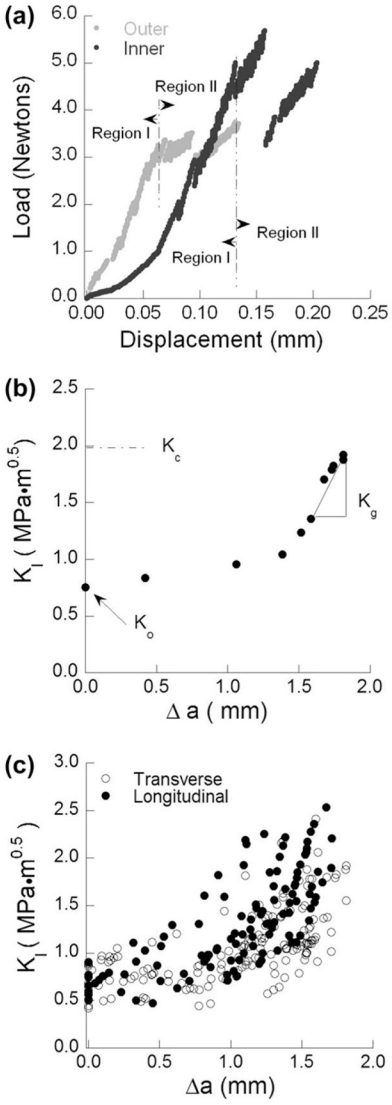

Fig. 3.

Stable crack extension in the inset CT enamel specimens. (a) Load vs. load-line displacement distributions obtained for specimens of inner and outer enamel during stable crack extension in the transverse direction. Region I denotes preloading and Region II distinguishes the portion of response associated with incremental crack extension. (b) Crack growth resistance curve (i.e. R-curve) for crack extension within the inner enamel. The quantities K_0, K_g and K_c represent the initiation toughness, growth toughness and fracture toughness, respectively. (c) R-curves for all specimens in the longitudinal and transverse directions.

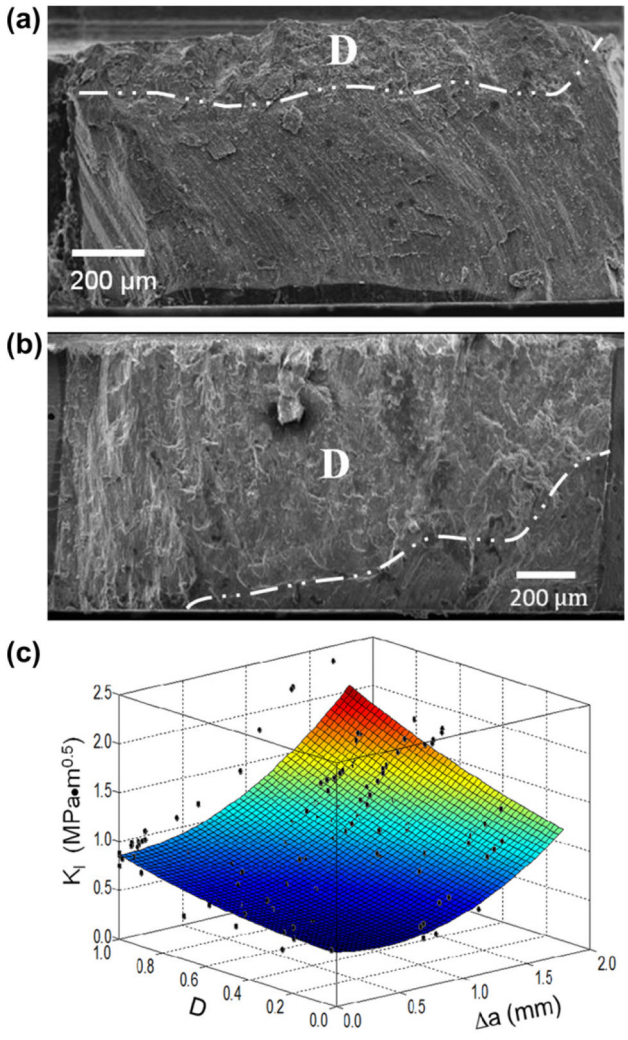

Fig. 4.

The role of degree of decussation on the crack growth resistance of enamel in the transverse direction. (a) Fracture surface of an enamel specimen with a low (D = 0.20) degree of decussation. (b) Fracture surface of an enamel specimen with a high (D = 0.85) degrees of decussation. Both micrographs in (a) and (b) have been annotated with a line demarcating the division between the decussated (D) and non-decussated zones on the fracture surfaces. Note that the direction of crack growth is from left to right. (c) Crack growth resistance of enamel in the transverse direction as a function of the degree of decussation.

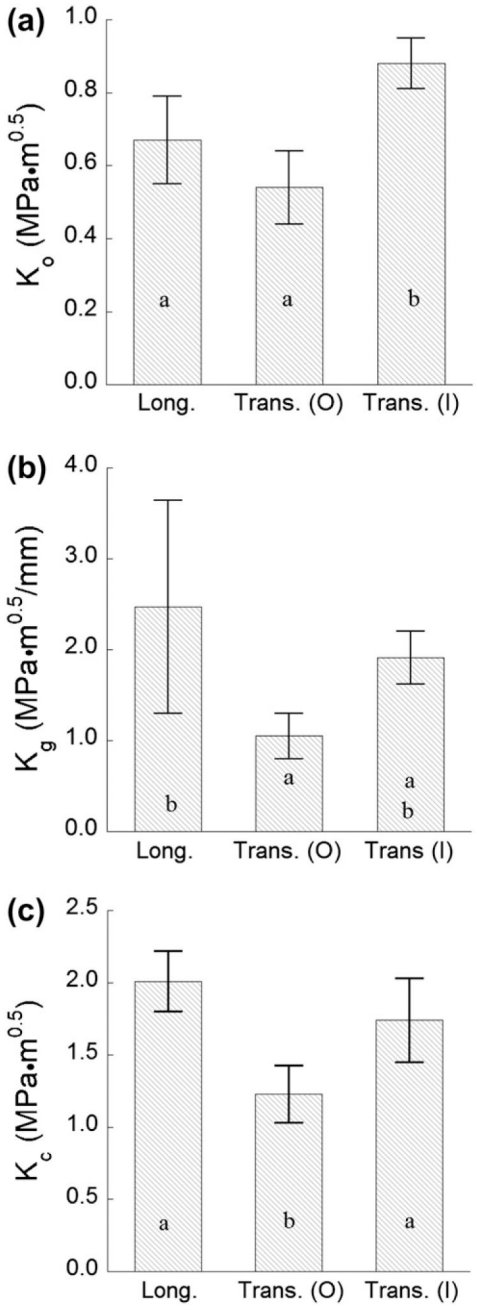

Fig. 5.

A comparison of the parameters quantifying the fracture behavior of enamel for crack growth in the longitudinal (Long.) and transverse (Trans.) directions. Responses for the transverse direction have been divided into two groups corresponding to the outermost enamel (O; $D \leq 30\%$) and the innermost enamel (I; $D \geq 70\%$). (a) The initiation toughness (K_0); (b) the growth toughness (K_g); and (c) the maximum crack growth resistance (i.e. the fracture toughness, K_c).

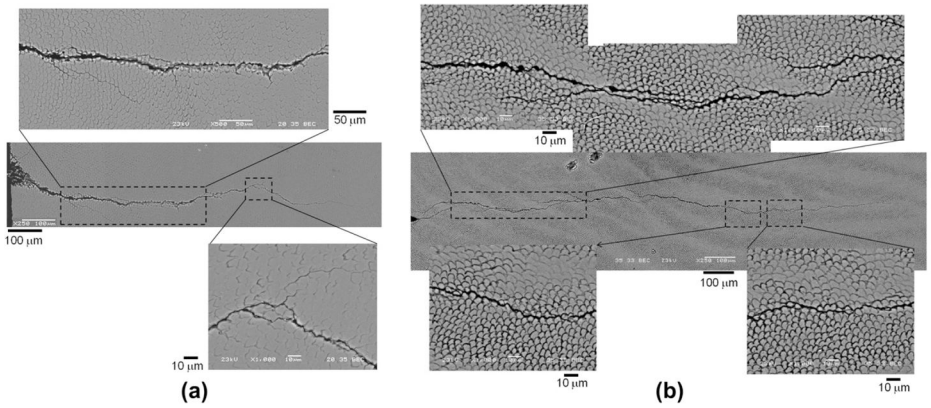

Fig. 6.
Crack path resulting from incremental crack growth from the notch in the transverse orientation. (a) Sample of outer enamel (female 19); (b) sample of inner enamel (female 21). Please see the online version of the manuscript for higher figure quality.

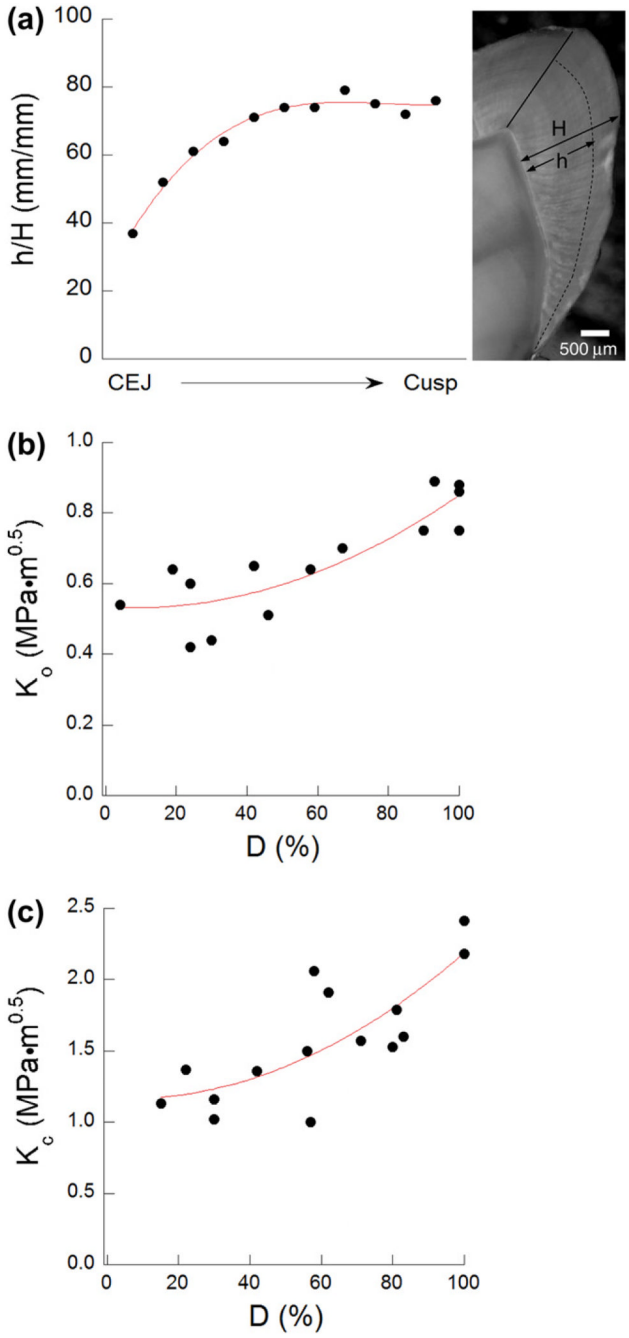

Fig. 7.

Degree of decussation and the fracture behavior. (a) Variation of the decussation ratio *h*/*H* for a third molar from the CEJ to the cusp. The parameters *h* and *H* are the decussated enamel and total enamel thickness at different regions, respectively. (b) Initiation toughness of enamel as a function of degree of decussation (*D*) in the transverse direction. (c) Fracture toughness of enamel as a function of degree of decussation (*D*) in the transverse direction.

Table 1

Comparison of the fracture behavior in the two directions of crack growth.

Parameter	**Crack growth direction**		
	Transverse	**Longitudinal**	***p*-value**
K_0 (MPa·m$^{0.5}$)	0.68 ± 0.16	0.67 ± 0.12	NS
K_g (MPa·m$^{0.5}$ mm^{-1})	1.59 ± 0.23	2.48 ± 1.20	$p \leq 0.05$
K_c (MPa·m$^{0.5}$)	1.67 ± 0.40	2.01 ± 0.21	$p \leq 0.01$
	Outer	*Inner*	
K_0 (MPa·m$^{0.5}$)	0.60 ± 0.14	0.81 ± 0.07	$p \leq 0.01$
K_g (MPa·m$^{0.5}$ mm^{-1})	1.37 ± 0.48	1.91 ± 0.26	$p \leq 0.05$
K_c (MPa·m$^{0.5}$)	1.47 ± 0.35	1.96 ± 0.28	$p \leq 0.01$